Influence of exciton-exciton interactions on the coherent optical response in GaAs quantum wells

K. Bott, O. Heller, D. Bennhardt, S. T. Cundiff, and P. Thomas
Department of Physics and Materials Sciences Center, Philipps University, D-35032 Marburg, Federal Republic of Germany

E. J. Mayer, G. O. Smith, R. Eccleston, and J. Kuhl
Max-Planck-Institut für Festkörperforschung, Heisenbergstrasse 1, D-70506 Stuttgart, Federal Republic of Germany

K. Ploog
Paul-Drude-Institut für Festkörperelektronik, D-10117 Berlin, Federal Republic of Germany
(Received 5 August 1993)

The degenerate-four-wave-mixing response of excitons in GaAs quantum wells is modeled using the optical Bloch equations including exciton-exciton interactions. The results display a strong dependence on the polarization of the excitation pulses. The model predicts intensity and polarization dependences of the time-integrated signal and characteristic temporal features of the time-resolved and time-integrated response in excellent agreement with observations.

I. INTRODUCTION

Transient four-wave-mixing (TFWM) experiments have been extensively used to study excitation dynamics in bulk GaAs and quantum wells (QW).[1] Recently, it has been observed that the TFWM signal exhibits unexpected dependences on the polarization of the incident fields,[2–6] which have been largely ignored in the past. These observed changes for linearly cross-polarized (CP) incident fields compared to parallel-polarized (PP) fields include an increase of the apparent dephasing rate,[2,4–6] phase shifting of quantum beats,[3] and a shift of the emission time to $t \approx \tau$ from $t = 2\tau$ for inhomogeneously broadened transitions.[2,5] Additionally, many of these features are observed to be surprisingly density dependent.[2,4] The theoretical treatment of TFWM is often based on the optical Bloch equations (OBE), which were developed to describe the nonlinear optical response in atomic systems.[7] A similar treatment, known as the semiconductor Bloch equations, was developed to describe the nonlinear optical response of semiconductors and shown to be equivalent to the OBE in certain limits.[8] This approach, including extensions, has been very successful in describing many features of the TFWM response.[9] However, the previously mentioned polarization dependences are not reproduced, although the introduction of disorder induced band mixing does provide agreement with certain features.[5] In the theoretical treatment presented here exciton-exciton interactions are included, providing excellent agreement with many of the experimentally observed polarization and density dependences. The theory is only developed for the TFWM signal emitted in the direction $2\mathbf{k}_2 - \mathbf{k}_1$ for incident pulses with wave vectors $\mathbf{k}_1$ and $\mathbf{k}_2$; extension to other geometries is straightforward.

Several recent experimental studies have demonstrated that exciton-exciton interactions are important and observable in TFWM experiments in GaAs QW's. The observations include dephasing due to exciton-exciton and exciton–free-carrier collisions,[10] coherent interactions,[9,11–13] and the formation of biexcitons.[14–19] Despite these observations, exciton-exciton interactions have in general not been included in theoretical models. In the theoretical treatment presented here the oppositely polarized excitons are combined into a single level scheme which includes one or more two-exciton states. The resulting level scheme then admits the inclusion of exciton-exciton interactions in a relatively straightforward and intuitive manner. This phenomenological model based on the optical Bloch equations represents a considerable simplification compared to a fundamental theory starting from the semiconductor Bloch equations. Our approach yields largely analytical expressions for the polarization dependence of the important parameters characterizing the TFWM-signal and provides a vivid interpretation of the experiments. The enormous potential of this simple model is demonstrated by the impressive agreement of its predictions with many of the features observed in previous experiments.[2–6] Earlier calculations of circularly polarized pump-probe results using this model have also provided good agreement with observations and shown in a much less general way that the model is equivalent to two two-level systems if no exciton-exciton interactions are present.[20] While calculations have also been performed based on a four-level "excitonic" picture, which was simply assumed to be the appropriate scheme,[6,15,21] they emphasized the explanation of certain experiments and did not include a detailed investigation of polarization and excitation density dependences of the TFWM signal. A different but related approach has been used in recent work which included excitation induced dephasing in calculations for the TFWM response in bulk GaAs, also providing good agreement with observations.[22] This approach appears to

 ©1993 The American Physical Society

give quite similar results to that presented here, although the formulations of the approaches themselves are different. Further theoretical work on the models is necessary to discover if there are clearly distinct predictions which can be experimentally observed.

The theoretical treatment is most transparent if only a single pair of transitions is considered, corresponding to excitation of only the heavy-hole (hh) exciton, as is presented in the following section. This is followed by a brief description of the experimental results, after which the theory is extended to include both the hh and light-hole (lh) excitons. This extension is in complexity only, not in substance, and allows comparison with the observed polarization dependences of the hh-lh beating.

II. TWO-EXCITON STATES

A. Theory

Near the band gap, the optical response of GaAs is dominated by the exciton resonance. Optical excitation of an exciton corresponds to promoting an electron from one of the two effective angular momenta $J = 3/2$ valence bands to the $J = 1/2$ conduction band. Due to momentum conservation, only the exciton composed of band states near $\mathbf{k} = \mathbf{0}$ need be considered, hence the conduction band can be accurately represented by a pair of $J_z = \pm 1/2$ states, and the valence band by a pair of $J_z = \pm 3/2$ (hh) and a pair of $J_z = \pm 1/2$ (lh) states. In a quantum well, confinement lifts the $\mathbf{k} = \mathbf{0}$ degeneracy between the hh and lh excitons. Additionally it provides a natural axis of quantization so that for incident fields perpendicular to the plane of the quantum well only transitions with $\Delta J_z = \pm 1$ are dipole allowed and are driven by oppositely circularly polarized components of the incident fields.

For simplicity we restrict the discussion in this section to hh excitons (experimentally this requires the use of incident fields of sufficiently narrow bandwidth to excite only the hh exciton). Usually the optical properties of the hh exciton are modeled in the frame of two independent two-level systems belonging to the different electron and hole spin states and excited by σ^+ and σ^- polarized light, respectively. We will designate the exciton excited by σ^+ (σ^-) polarized light, consisting of a $J_z = -1/2$ ($+1/2$) electron and $J_z = +3/2$ ($-3/2$) hole, as a σ^+ (σ^-)-exciton. Quantum mechanically these independent σ^+- and σ^--excitons are described in two-dimensional single particle Hilbert spaces $\mathcal{H}_+^{(1)}$ and $\mathcal{H}_-^{(1)}$. The physical behavior of the two noninteracting particles can also be treated in a two-particle Hilbert space. Since the σ^+ and σ^- excitons are distinguishable, the two-particle Hilbert space is given by the direct product of the one-particle Hilbert spaces

$$\mathcal{H}^{(2)} = \mathcal{H}_+^{(1)} \otimes \mathcal{H}_-^{(1)} .$$

Operators $A_\pm$ acting in $\mathcal{H}_+^{(1)}$ and $\mathcal{H}_-^{(1)}$ are extended by

$$A = (A_+ \otimes E_-) + (E_+ \otimes A_-) ,$$

where $E_\pm$ are the unit operators in $\mathcal{H}_\pm^{(1)}$.[23] The Hilbert space $\mathcal{H}^{(2)}$ consists of four levels (see Fig. 1), the ground state (no excitation), two single-exciton states (either the σ^+ or the σ^- exciton is excited), and the two-exciton state (the σ^+ and the σ^- exciton are excited simultaneously but do not interact).

The two two-level systems and the four-level system provide a completely equivalent description of two noninteracting excitons if both the matrix elements μ, ν and the dephasing rates γ_μ, γ_ν for the transitions from the ground- to the single-exciton states and from the single-exciton states to the two-exciton state are exactly equal and if the energy of the two-exciton state is twice the energy of the single-exciton state. Experiments performed with linearly polarized excitation pulses are better discussed in terms of the four-level scheme depicted in the lower right part of Fig. 1, which can be shown to be equivalent to the uncoupled two-level systems and is obtained from the scheme in the upper right-hand part by a simple basis transformation.

In the four-level system it is clear that exciton-exciton interactions can now be easily included by breaking the equivalence between the lower two and upper two transitions. This is due to the fact that the lower transitions represent excitations out of the ground state by the applied field acting first in perturbation, whereas the upper

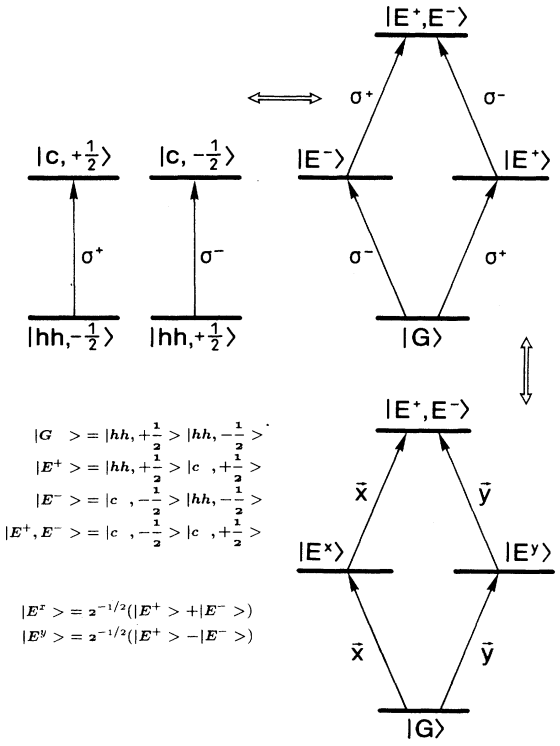

FIG. 1. Level schemes for circularly polarized hh exciton transitions in a $GaAs/Al_xGa_{1-x}As$ quantum well. The upper left and right parts are equivalent to describe the σ^+ and σ^- excitons in two one-particle Hilbert spaces or in one two-particle Hilbert space. The lower part depicts the selection rules for linearly polarized light in the four-level scheme.

transitions only contribute if there are already optically induced excitations, so that their parameters will include dynamics due to interaction with these excitations. Such dynamics can include dephasing due to exciton-exciton collisions, resulting in a higher dephasing rate for the upper transitions, and biexcitonic effects, resulting in a shifting of the energy of the two-exciton state. This modified system is depicted in Fig. 2, where Δ represents the energy shift of the two-exciton state.

The TFWM signal is calculated for this modified system by deriving the appropriate OBE from the master equation for the density matrix and iterating to third order within the rotating wave approximation. There are two classes of terms which contribute to the signal emitted in the correct direction for a self-diffracted two pulse TFWM experiment (i.e., $2\mathbf{k}_2-\mathbf{k}_1$, where $\mathbf{k}_1$ and $\mathbf{k}_2$ correspond to the directions of the two excitation pulses). The iteration path for terms in the first class goes through a diagonal element of the density matrix to second order. These terms only contribute when the pulse with wave vector $\mathbf{k}_1$ arrives first in time. The iteration path for terms in the second class goes through an off-diagonal element (i.e., coherence) to second order. These terms only contribute when the pulse with wave vector $\mathbf{k}_2$ arrives first. Additionally the second set of terms cancels for the unmodified four-level-system, as they must because they cannot exist in the two-level systems. The coherence at second order decays at a rate γ_{2ex}, which is a free parameter in our calculation. A complete microscopic theory must relate γ_{2ex} to the rates γ_μ and γ_ν.

In the short pulse (δ-function) limit the OBE can be analytically solved for the induced third order polarization $\mathbf{P}^{(3)}_{2\mathbf{k}_2-\mathbf{k}_1}(t,\tau)$ as a function of time, t, and delay between the pulses, τ (positive for the pulse corresponding to $\mathbf{k}_1$ arriving first), which radiates in the direction $2\mathbf{k}_2-\mathbf{k}_1$. The time-integrated signal intensity $I(\tau)$ is given by the formula

$$I(\tau)=\int_{-\infty}^{+\infty}|\mathbf{P}^{(3)}_{2\mathbf{k}_2-\mathbf{k}_1}(t,\tau)|^2\,dt \tag{1}$$

assuming that there is no polarization orientation analysis in the detection. Inserting the results of the OBE yields

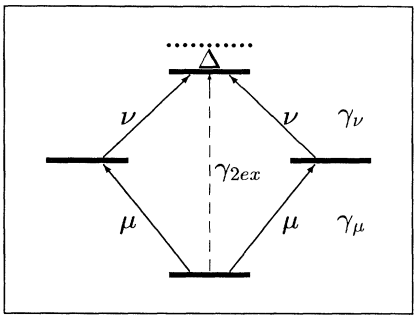

FIG. 2. The renormalized four-level-system which may describe exciton-exciton interactions by choosing $\mu\neq\nu$, $\gamma_\mu\neq\gamma_\nu$, or $\Delta\neq 0$. μ and ν, denote the transition matrix elements, γ_μ and γ_ν dephasing rates, and Δ the biexciton binding energy.

$$\begin{aligned} I(\tau)= \quad & \Theta(-\tau)\,\exp(+2\tau\,\gamma_{2ex})\times 2\mu^4\nu^4\left[\gamma_\mu^{-1}+\gamma_\nu^{-1}-4\frac{\gamma_\mu+\gamma_\nu}{(\gamma_\mu+\gamma_\nu)^2+\Delta^2}\right] \\ & +\Theta(+\tau)\,\exp(-2\tau\,\gamma_\mu)\times\left[2\mu^4\nu^4\gamma_\nu^{-1}+\cos^2\theta_{12}\left(8\mu^8\gamma_\mu^{-1}-16\mu^6\nu^2\frac{\gamma_\mu+\gamma_\nu}{(\gamma_\mu+\gamma_\nu)^2+\Delta^2}\right)\right], \end{aligned} \tag{2}$$

where θ_{12} is the angle between the electric field vectors of the incident linearly polarized fields and the other parameters are defined in Fig. 2. Terms which contribute only for delays such that the pulses overlap in time are ignored in this expression.

Examination of Eq. (2) reveals that the signal consists of two terms, the first only contributes for $\tau<0$, while the second contributes for $\tau>0$. These terms can be associated with the two classes of iteration paths described earlier. This suggests that the first, $\tau<0$ term is characteristic of exciton-exciton interactions, and indeed it vanishes for $\Delta=0$ and $\gamma_\mu=\gamma_\nu$. Earlier observations of the presence of a signal for $\tau<0$ in TFWM experiments have also been attributed to exciton-exciton interactions.[9,11]

The strength of the second term ($\tau>0$) exhibits a $\cos^2\theta_{12}$ dependence on θ_{12}, the angle between the polarization vectors of the two optical fields. As this dependence disappears for $\mu=\nu$, $\gamma_\mu=\gamma_\nu$, and $\Delta=0$; it is also a consequence of exciton-exciton interaction.

Although there does exist an energy splitting (Δ) in the model, corresponding to the biexciton binding energy, this does not result in the appearance of any form of beating for this experimental configuration. Earlier observations have attributed the presence of beats[15,24] to biexcitonic effects, however the corresponding theoretical analysis required the introduction of asymmetric pulses into a similar model.[21]

The polarization dependence of the signal intensity given by Eq. (2) becomes more transparent if we choose the limit where τ approaches 0 from the positive side ($\tau=0^+$). Experimentally this corresponds to a fixed delay which is larger than the pulse width, but much smaller than the relevant decay times. In this limit, and defining some constants, we obtain the signal intensity and polarization angle, θ_{sig},

$$I(\tau=0^+)\propto\Gamma_1+\cos^2\theta_{12}(2\Gamma_2-2\Gamma_3)\,, \tag{3}$$

$$\theta_{sig}=-\frac{1}{2}\arctan\left(\frac{\sin(2\theta_{12})(\Gamma_1-\Gamma_3)}{\Gamma_3-\Gamma_2+\cos(2\theta_{12})(\Gamma_3-\Gamma_2-\Gamma_1)}\right) \tag{4}$$

with

$$\Gamma_1 = \frac{\nu^4}{\gamma_\nu}\ , \quad \Gamma_2 = 2\frac{\mu^4}{\gamma_\mu}\ , \quad \Gamma_3 = 4\mu^2\nu^2\frac{\gamma_\mu+\gamma_\nu}{(\gamma_\mu+\gamma_\nu)^2+\Delta^2}\ .$$

The dependence of these quantities on θ_{12} is displayed in Figs. 3(a), and 3(b) for several sets of parameters. This dependence is very similar to the experimental data described below.

The density dependence of the exciton-exciton interactions will result in the parameters in Eqs. (3) and (4) being density dependent, and hence we can associate the different curves in Fig. 3 with different densities. Assuming that the density dependence of the exciton-exciton interactions is primarily manifested in a change in the ratio of the dephasing rates for the lower transitions to that for the upper transitions $\frac{\gamma_\mu}{\gamma_\nu}$, and that increasing density corresponds to a decrease in the ratio, we associate the solid curve with low density and dashed and dotted curves with increasingly higher densities. An experimental determination of these parameters is difficult and requires a detailed study of dephasing rate dependence on density. It is physically very reasonable that the ratio of dephasing rates does display a density dependence as contributions of various incoherent exciton-exciton interaction mechanisms, such as screening and exciton-exciton collisions, will change in importance with respect to each other and with respect to other dephasing mechanisms (disorder, phonons, etc.) as the density changes. The requirement that the ratio of the dephasing rates $\frac{\gamma_\mu}{\gamma_\nu}$ decreases with increasing density corresponds specifically to a decrease in the slope of the dephasing rate as a function of density, which has been predicted theoretically.[25]

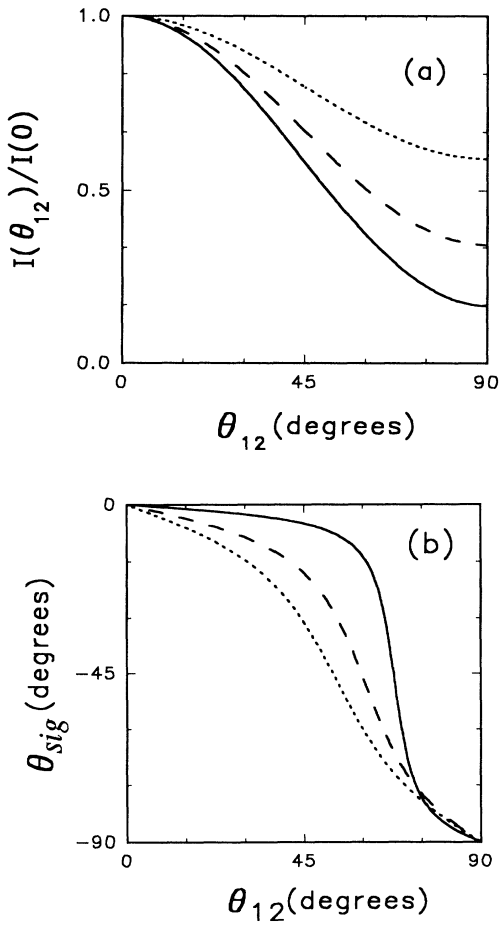

FIG. 3. (a) Theoretical curves for the intensity of the TFWM signal $I(\tau = 0^+)$ vs θ_{12} for the parameter set $\mu = 1$, $\nu = 1$, Δ =0.15 meV, and $\gamma_\mu^{-1} = 12$ ps, $\gamma_\nu^{-1} = 6$ ps (solid line); $\gamma_\mu^{-1} = 6$ ps, $\gamma_\nu^{-1} = 4.5$ ps (dashed line); $\gamma_\mu^{-1} = 4$ ps, $\gamma_\nu^{-1} = 4$ ps (dotted line). (b) Maximum of the polarization angle of the DFWM signal $\theta_{\rm sig}$ at delay $\tau = 0^+$ vs θ_{12} . Theoretical curves with the same parameters as in (a).

Making this association between the curves in Fig. 3 with increasing density agrees very well with the density dependence of the experimental observations presented in the following section. It is interesting to note that at high density the signal intensity becomes less sensitive to the polarization of the incident fields, and the signal's polarization angle approaches $\theta_{\rm sig} = -\theta_{12}$; both are the result expected from the uncoupled two-level system model.

B. Experimental results

The excitation pulses were generated by a mode-locked Ti:sapphire laser system operating at a repetition rate of 76 MHz and providing transform-limited pulses as short as 150 fs. For many experiments the pulse duration was increased to approximately 1 ps by external spectral filtering of the output in order to suppress simultaneous excitation of the continuum. This is necessary because free electrons and holes rapidly dephase free excitons even at modest excitation levels. For time-resolved experiments an additional reference pulse was derived from the output of the same laser system.

For these experiments, we used the two-pulse self-diffraction backward (reflection) geometry. The polarization of the input pulses was adjusted by and the polarization of the time-integrated signal was analyzed by Glan-Thompson polarizers and a $\lambda/2$ plate providing polarization definition of better than 200:1. The time-integrated signal was detected by a cooled GaAs photomultiplier or a Si-photodiode. Time resolution of the diffracted signal (see Sec. III B) at a fixed delay τ is accomplished by up-conversion of the signal with a reference pulse in a 2-mm-thick $LiIO_3$ crystal. The up-converted signal is monitored by a cooled GaAs-photomultiplier as a function of the time delay of the reference pulse.

The time-integrated experiments were performed on a 27 nm GaAs single QW which has a 0.2 meV hh exciton linewidth and no measurable shift ($\leq$ 0.02 meV) between PL and PLE spectra. To avoid strain the sample is not etched, necessitating the use of the reflected TFWM geometry. The samples were mounted in a continuous-flow helium cryostat and maintained at temperatures between 5 and 8 K.

In Fig. 4(a) the measured intensity of the TFWM signal at a fixed small delay is plotted as a function of θ_{12} for various densities between 3.1×10^8 cm^{-1} and 7.4×10^9 cm^{-1}. Spectrally narrow pulses are used so that only the

hh exciton is resonantly excited. At low densities, the functional form [see solid line in Fig. 4(a)] follows that derived from the model and plotted in Fig. 3(a). The density dependence is also qualitatively similar to the theoretical predictions although the experimental data show deviations from a $\cos\Theta_{12}$ law at higher densities. In Fig. 4(b) the measured θ_{sig} is plotted as a function of θ_{12} for densities of 4×10^8 cm^{-1} and 4×10^9 cm^{-2}. Again the measurements closely match the theoretical predictions in Fig. 3(b).

It should be noted that the phenomenological introduction of the density dependence for the parameter μ, ν, γ_μ, γ_ν, and Δ in Eqs. (3) and (4) discussed in the previous section has tacitly assumed that the exciton-exciton interaction strength or scattering rate remains approximately constant during the experiment. This presumption corresponds to experiments which are performed with low excitation pulses and where the scattering rate is varied by injection of a prepulse with a suitable intensity. This technique has been employed in Refs. 10, 22, and 26. To the contrary, the exciton density in the experiments depicted in Fig. 4 was altered by varying the intensity of the two pulses applied for the TFWM experiment. A theoretically correct description of such an experiment principally requires consideration of higher order (>3) contributions to the nonlinear polarization. Instead we have confined our calculation of the polarization to 3rd order terms and used an average exciton density. This treatment contains an additional approximation, but the model provides a qualitative explanation of the experimentally observed variation of the signal's peak intensity and polarization as a function of the angle θ_{12} with excitation density.

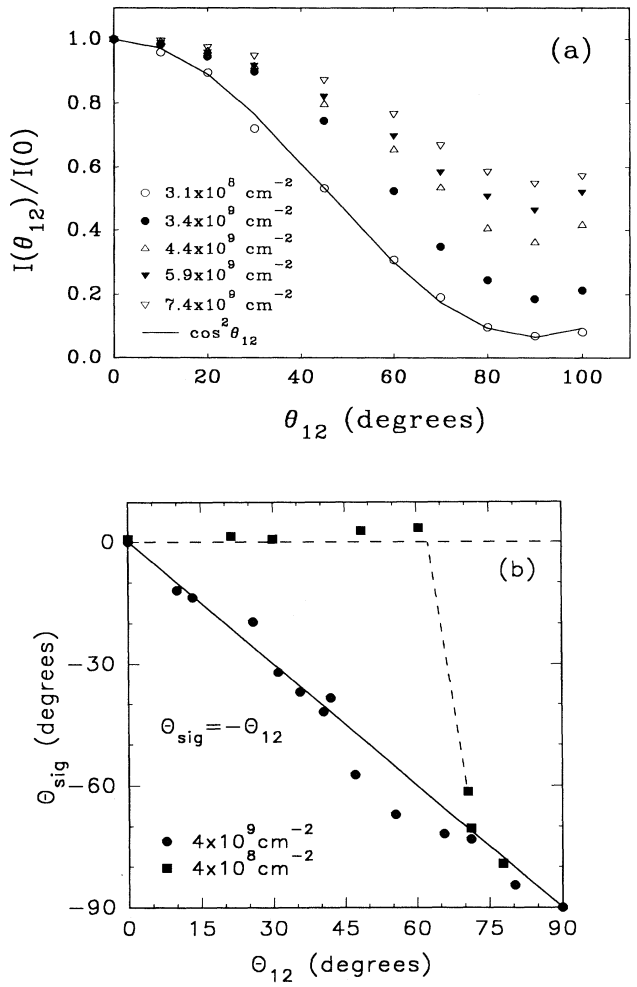

FIG. 4. Experimental data corresponding to Fig. 3 measured on a 27 nm $GaAs/Al_{0.3}Ga_{0.7}As$ single QW for different excitation densities. (a) Normalized signal intensity at $\tau = 0^+$ vs θ_{12}; (b) Polarization angle of the signal vs θ_{12}. The solid line depicts the relation $\Theta_{sig} = -\Theta_{12}$ expected for two uncoupled two-level systems, the dashed horizontal line represents $\Theta_{sig} = 0$, the oblique dashed line marks a region where the signal is almost unpolarized.

III. EXTENSION TO THREE-LEVEL SYSTEMS

A. Theory

Incident fields of sufficient spectral bandwidth can excite both the hh and lh excitonic resonances resulting in the observation of quantum beats in the TFWM signal. While quantum beats have been observed in many semiconductor systems[1] including lh-hh quantum beats in time-integrated TWFM (Refs. 27 and 28) and time-resolved TFWM,[29] most of these measurements have ignored their polarization dependence. The basic feature of a 180° phase shift of the beats between PP and CP polarization has been successfully explained by a model which consists essentially of two uncoupled three-level systems.[3] By using the technique described above to convert these two three-level systems into a single nine-level system, exciton-exciton interaction can now be included.

Analytic calculations are performed on this nine-level system, which is depicted in Fig. 5 and consists of one ground-state, four exciton states (σ_+ and σ_-, hh and lh states), and four two-exciton states (one two-hh state, one two-lh state, and two hh-lh states), in exactly the same manner as described above for the four-level system.

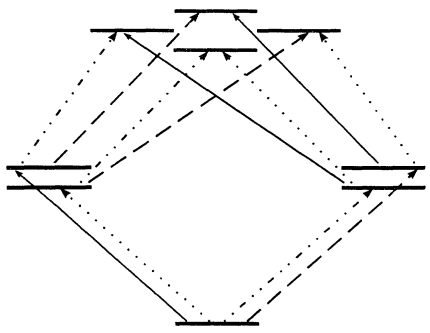

FIG. 5. Nine-level-scheme for description of circularly polarized lh- and hh- exciton transitions in a QW consisting of one ground state, four single-exciton, and four two-exciton states. (For further details see text.)

There exist 12 dipole allowed transitions of four distinct types which correspond to the excitation of a σ_- lh exciton (solid arrows in Fig. 5), excitation of a σ_+ lh exciton (dashed), excitation of a σ_+ hh exciton (dotted), and excitation of a σ_- hh exciton (dashed/dotted). Exciton-exciton interactions are introduced in exactly the same manner as above, by breaking the symmetry between the ground-state to exciton transitions and the exciton to two-exciton transitions. The analytic results of the calculation are lengthy, and greater insight is obtained by examining the results for a few typical cases.

The calculated time-integrated TFWM signal for this nine-level system is shown in Fig. 6 as a function of τ including exciton-exciton interactions. As expected, the inclusion of both hh and lh states results in the appearance of quantum beats; however, a striking new feature is the appearance of quantum beats on the rising edge of the signal, i.e., for negative delays. This is consistent with previous experimental observations[27,28] and with the data presented in the following section. As for the four-level system, a signal for negative delays only occurs when exciton-exciton interactions are included in the model. The slope of this rising edge is determined by the dephasing rate of the coherence between the two-exciton state and the ground state. While in general this rate should be calculated microscopically, in the simplest approximation it will be the sum of the dephasing rates for the two single-exciton states which make up the two-exciton states, resulting in a dephasing rate twice that of the single-exciton states. As a consequence, the rising edge exhibits a slope twice that of the decay for positive delays, as the decay is determined by the dephasing of the single-exciton states.

At zero delay the calculated signal exhibits features which arise due to the distinct origins of the signals for negative and positive delays. The PP and CP signals exhibit differing features: in the PP case there is an abrupt rise at $\tau = 0$ (which is accentuated in the calculation by the δ-function pulse limit), while for the CP case a drop at $\tau = 0$ occurs. These features also appear quite clearly in the experimental observations.

Many experimental observations have also shown that the beat amplitudes differ for the PP and CP cases. The model presented here reproduces this if the dephasing rates for the two-exciton states, which represent a combination of a hh and lh exciton, are assumed higher than those for the states which are purely hh or lh in nature. A complete justification of such a distinction requires a more complete understanding of the microscopic origin

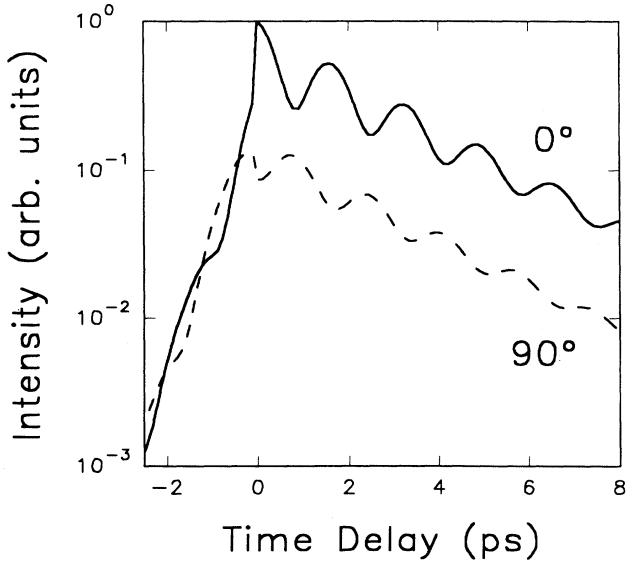

FIG. 6. Theoretical calculation of the time-integrated TFWM signal versus delay time in the nine-level scheme including exciton-exciton interaction.

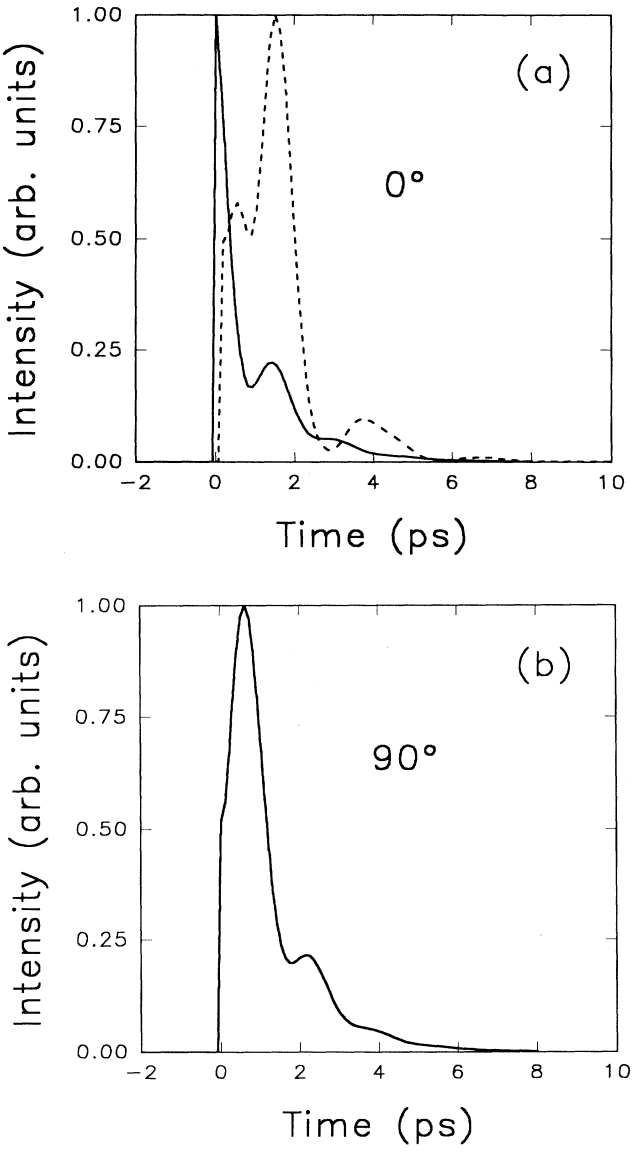

FIG. 7. Theoretical time-resolved TFWM signal generated at $\tau = 0$ for parallel (a) and cross polarized excitation (b). In (a) the solid and dashed curves are calculated for $\Delta = 0$ and 1.5 meV, respectively. In (b) the signal shape is independent of Δ.

of the dephasing.

The observed difference in signal intensity for PP versus CP arises in a similar manner to that described above for a four-level system, however there is a larger number of parameters which contribute for the nine-level system. As a consequence there is a range of physically reasonable parameters for which the model provides a reasonable reproduction of the observations. In light of this Fig. 6 is presented primarily for illustrative purposes, and determination of a complete set of unique parameters will require extensive experimental measurements to isolate as many individual parameters as possible. The parameters for Fig. 6 do include a nonzero shift of the upper states and, as for the four-level system, no beating corresponding to this energy shift is observable.

A beat which corresponds to the energetic shift, Δ, of the upper states due to biexcitonic effects is not evident in the time-integrated signal, and in general a close fit to the experimental results can be achieved without the introduction of such a shift. The opposite is true for the time-resolved signal: Fig. 7 shows the time-resolved signals for $\Delta = 0$ (solid line) and $\Delta = 1.5$ meV (dashed line) at $\tau = 0$ for the PP (a) and CP (b) configuration. It is clear that the introduction of a nonzero Δ dramatically modifies the PP signal. Although it is not immediately obvious from these figures, this change is due to beating with a frequency which corresponds to Δ. With $\Delta = 0$ the time-resolved signal consists of quantum beating corresponding to the hh- lh splitting with a 180° phase shift between PP and CP, as predicted using uncoupled three-level systems.[3] Inclusion of a biexcitonic binding energy shifts the maximum signal for the PP away from t=0, but not for the CP case. This modification is consistent with the experimental observations presented in the following section.

The inclusion of self-interaction terms (called local-field or polarization-wave interaction) has been shown to result in similar modifications of the time-resolved signal.[9,12,13] Because the emphasis of the model developed here is on exciton-exciton interaction between excitons of opposite spin, which is most naturally incorporated in this model, such self-interactions are not currently included. This means that the experimental observations of such a shift in the signal maximum cannot be taken as conclusive evidence that the model applies, but should be only considered as consistent with the model.

B. Experimental results

For comparison with the predictions of the nine-level model, we have performed time-integrated PP and CP TFWM experiments on a multiple QW with ten periods of 25 nm GaAs and 30 nm $Al_{0.3}Ga_{0.7}As$. For these experiments, the substrate was removed by polishing and etching, and the signal was measured in the forward diffraction geometry. Figure 8 shows the time-integrated TFWM signal measured for both PP and CP cases. Besides a significantly faster dephasing rate for the CP geometry and a 180° phase shift of the quantum beats, the curves exhibit an abrupt increase at zero delay for the PP

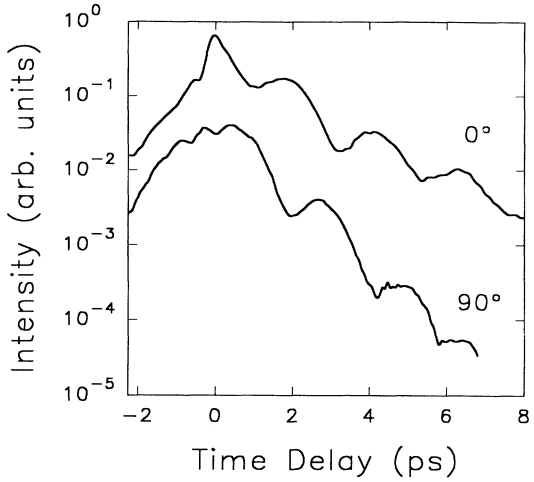

FIG. 8. Experimental time-integrated results measured for parallel and cross polarized beams on a MQW with ten periods of 25 nm GaAs and 30 nm $Al_{0.3}Ga_{0.7}As$.

geometry, and in the CP geometry an additional dip is apparent near zero delay. Besides the remarkable differences in the signal decay rate for the CP geometry, which can be attributed to disorder-induced coupling between the excitonic states in our inhomogeneously broadened sample,[5] comparison of these experimental curves with

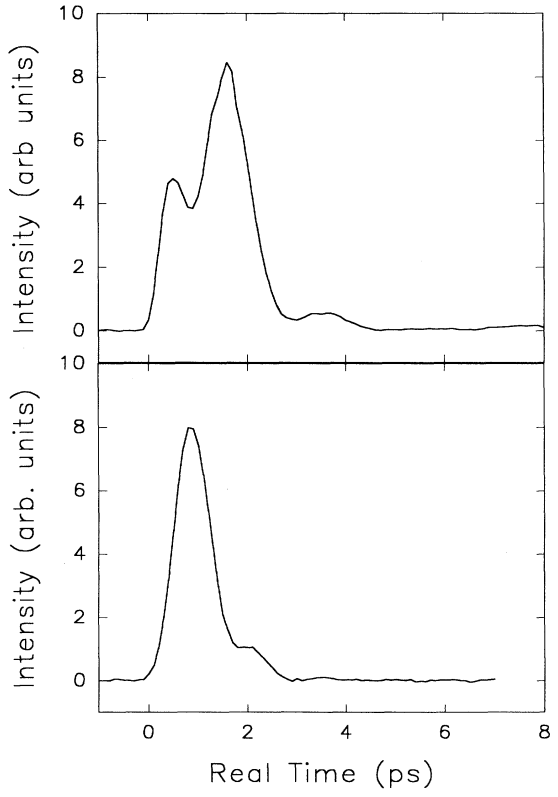

FIG. 9. Experimental time-resolved TFWM signal observed at τ=0 for parallel (upper part) and perpendicular polarization (lower part) on the MQW used also in Fig. 8.

the theoretical traces in Fig. 6 demonstrates impressive agreement if one takes into account that the finite pulse duration implies a smoothing of the experimental signal structures in the pulse overlap region.

Figure 9 depicts time-resolved shapes of the TFWM signal created for time-delay zero between the two excitation fields. The PP signal shows a well resolved secondary maximum on the rising edge, which is clearly not present in the CP case. These data agree quite well with the theoretical results presented in Fig. 7, which include $\Delta \neq 0$. As noted above, this agreement cannot be taken as conclusive evidence that true bound biexcitons are necessary to explain the observations as coherent self-interactions may lead to similar results. However, in either case it is clear that exciton-exciton interactions are necessary to explain the polarization dependence of the time-resolved signal.

IV. CONCLUSIONS

We have theoretically demonstrated that the two two-level transitions, which are generally used to describe the two opposite spin hh exciton transitions in a QW, can be recast into an equivalent four-level system. Similarly the three-level systems, which are generally employed to include the lh transitions, can be recast into a nine-level system. While calculations for the TFWM response with the OBE derived from these transformed systems provide identical results to the original systems, they readily allow the inclusion of exciton-exciton interactions. Exciton-exciton interactions are included by modifying the matrix elements, dephasing rates, or energies corresponding to transitions between one-exciton and two-exciton states with respect to those for the transitions between the ground state and one-exciton states. Time-integrated and time-resolved TFWM measurements for excitation of the hh excitonic transitions alone and excitation of both hh and lh transitions are also presented. The dependence of the observations on the polarization of the incident fields is in excellent agreement with model calculations which include exciton-exciton interactions. As this model only includes interactions between opposite spin excitons, and certain aspects of the data may be explained by self-interactions alone, work is currently in progress to extend the model by including self-interactions so that the relative contributions can be determined. Additionally, extension of the model to include inhomogeneous broadening of arbitrary correlation may successfully describe not only all the polarization properties described herein, but also the observed dependence of the dephasing rate on polarization.[5,30] Although these developments are required to obtain a complete model which can describe all the experimental observations, the results presented in this paper clearly demonstrate that the inclusion of two-exciton states and exciton-exciton interactions is crucial to understanding the polarization dependences of the TFWM signal from two-dimensional excitons.

ACKNOWLEDGMENTS

The authors acknowledge many discussions with S.W. Koch, D.G. Steel, Y. Z. Hu, R. Binder, H. Wang, and J. Feldmann. One of authors (S.T.C.) acknowledges support from the Alexander von Humboldt Foundation.

[1] See, for example, *Optics of Semiconductor Nanostructures*, edited by F. Henneberger, S. Schmitt-Rink, and E. O. Göbel (Akademie Verlag, Berlin, 1993).
[2] S. T. Cundiff, H. Wang, and D. G. Steel, Phys. Rev. B **46**, 7248 (1992).
[3] S. Schmitt-Rink, D. Bennhardt, V. Heuckeroth, P. Thomas, P. Haring, G. Maidorn, H. Bakker, K. Leo, D.-S. Kim, J. Shah, and K. Köhler, Phys. Rev. B **46**, 10 460 (1992).
[4] R. Eccleston, J. Kuhl, D. Bennhardt, and P. Thomas, Solid State Commun. **86**, 93 (1993).
[5] D. Bennhardt, P. Thomas, R. Eccleston, E. J. Mayer, and J. Kuhl, Phys. Rev. B **47**, 13 485 (1993).
[6] H. H. Yaffe, Y. Prior, J. P. Harbison, and L. T. Florez, J. Opt. Soc. Am. B **10**, 578 (1993).
[7] See, for example, S. Stenholm, *Foundations of Laser Spectroscopy* (Wiley, New York, 1984).
[8] M. Lindberg and S. W. Koch, Phys. Rev. B **38**, 3342 (1988).
[9] M. Wegener, D. S. Chemla, S. Schmitt-Rink, and W. Schäfer, Phys. Rev. A **42**, 5675 (1990).
[10] A. Honold, L. Schultheis, J. Kuhl, and C.W. Tu, Phys. Rev. B **40**, 6442 (1989).
[11] K. Leo, M. Wegener, J. Shah, D. S. Chemla, E. O. Göbel, T. C. Damen, S. Schmitt-Rink, and W. Schäfer, Phys. Rev. Lett. **65**, 1340 (1990)
[12] S. Weiss, M.-A. Mycek, J.-Y. Bigot, S. Schmitt-Rink, and D.S. Chemla, Phys. Rev. Lett. **69**, 2685 (1992).
[13] D.-S. Kim, J. Shah, T. C. Damen, W. Schäfer, F. Jahnke, S. Schmitt-Rink, and K. Köhler, Phys. Rev. Lett. **69**, 2725 (1992).
[14] B. F. Feuerbacher, J. Kuhl, and K. Ploog, Phys. Rev. B **43**, 2439 (1991).
[15] S. Bar-Ad and I. Bar-Joseph, Phys. Rev. Lett. **68**, 349 (1992).
[16] D. J. Lovering, R. T. Phillips, G. J. Denton, and G. W. Smith, Phys. Rev. Lett. **68**, 1880 (1992).
[17] R. T. Phillips, D. J. Lovering, G. J. Denton, and G. W. Smith, Phys. Rev. B **45**, 4308 (1992).
[18] K.-H. Pantke, D. Oberhauser, V. G. Lyssenko, J. M. Hvam, and G. Weimann, Phys. Rev. B **47**, 2413 (1993).
[19] D. R. Wake, J. C. Kim, and J. P. Wolfe, in *Quantum Electronics and Laser Science Conference*, 1993 Postdeadline Papers (Optical Society of America, Washington, D.C., 1993), QPD21-1/46.
[20] S. T. Cundiff, Ph.D. thesis, University of Michigan, 1992.
[21] G. Finkelstein, S. Bar-Ad, O. Carmel, I. Bar-Joseph, and Y. Levinson, Phys. Rev. B **47**, 12 964 (1993).
[22] H. Wang, K. Ferrio, D.G. Steel, Y. Z. Hu, R. Binder, and S.W. Koch, Phys. Rev. Lett. **71**, 1261 (1993).
[23] A detailed description of this transformation can be found in, e.g., C. Cohen-Tannoudji, B. Diu, and F. Laloë, *Quan-*

tum Mechanics (Wiley, New York, 1977), pp. 386–475.
[24] O. Carmel and I. Bar-Joseph, Phys. Rev. B **47**, 7606 (1993).
[25] Y. Z. Hu, R. Binder, and S. W. Koch, in *Quantum Electronics and Laser Science Conference*, 1993 OSA Technical Digest Series, Vol. 12 (Optical Society of America, Washington, D.C., 1993), pp. 182 and 183; Phys. Rev. B **47**, 15 679 (1993).
[26] L. Schultheis, J. Kuhl, A. Honold, and C.W. Tu, Phys. Rev. Lett. **57**, 1635 (1989).
[27] B. F. Feuerbacher, J. Kuhl, R. Eccleston, and K. Ploog, Solid State Commun. **74**, 1279 (1990).
[28] K. Leo, T. C. Damen, J. Shah, E. O. Göbel, and K. Köhler, Appl. Phys. Lett. **57**, 19 (1990).
[29] M. Koch, J. Feldmann, G. von Plessen, E. O. Göbel, P. Thomas, and K. Köhler, Phys. Rev. Lett. **69**, 3631 (1992).
[30] T. Saiki, M. Kuwata-Gonokami, T. Matsusue, and H. Sakaki, in *Quantum Electronics and Laser Science Conference*, 1993 OSA Technical Digest Series, Vol. 12 (Optical Society of America, Washington, D.C., 1993), pp. 180 and 181.